

Mammographic Density Classification based on Local Histograms

Rafael Llobet¹, Juan A. Solves¹, Juan C. Perez-Cortes¹ and Francisco Ruiz-Perales²

¹ Instituto Tecnológico de Informática
Universidad Politécnica de Valencia, Camino de Vera s/n, 46071 Valencia, Spain

² Consellería de Sanitat. Comunitat Valenciana, Valencia, Spain

Abstract. In this work, the task of classifying mammograms according to breast density is studied using a local-histogram-based feature extraction method and a non-parametric classification scheme. Breast density estimation is important due to its association with a higher risk of cancer and an increased difficulty of diagnosis. 322 images from the Mammographic Image Analysis Society (MIAS) Database have been analyzed, and the density prediction accuracy of the method has been assessed. The obtained results show an agreement of 77.96% between automatic and expert radiologist manual classification.

1 Introduction

Breast cancer is a leading cause of cancer-related mortality in women. Some studies have estimated that approximately 12.6% of women will develop breast cancer during their lifetime [1]. Early detection of cancer is extremely important as only an early treatment will cure the disease in a significant number of cases.

Mammographic screening programs are currently an effective method to detect breast cancer at an early stage, because they allow the identification of tumors before being palpable. Nevertheless, it is not trivial for a radiologist to interpret correctly a mammogram due to the extremely wide variation in the mammographic appearance of normal and abnormal tissue of the breast. In fact, only 15 to 35% of women with radiographically-suspicious non-palpable lesions who are subject to a biopsy, show malignancy after histological analysis [2, 3]. On the other hand, some incipient tumors can remain undetected after a radiography has been examined, which makes difficult a successful treatment. Retrospective studies have shown that, in current breast cancer screening, 10% to 25% of the tumors are missed by the radiologist [4, 5].

In case of dense breasts, the diagnosis is even more difficult, because dense tissue has similar X-ray attenuation than some type of tumors. Therefore, dense breast tissue can obscure a lesion. In addition to the difficulty involved in the detection of certain types of tumors in dense breasts, some studies have demonstrated a correlation between dense tissue and the risk of developing cancer [6–8]. The risk of breast cancer associated with mammographic density is larger than almost all other risk factors for the disease. Women with dense breasts are at four-to-six-fold higher risk than those with primarily fatty breasts [9, 10, 8].

Since the discovery of this relationship, several metrics for breast density classification have been proposed: Wolfe's four parenchymal patterns [6, 7], Tabar's five patterns [11], Boyd's six class categories [8] and BI-RADS [12].

Regardless of the method employed to classify and estimate the mammographic density, this measure is of major importance as it could influence the choice of alternative screening paradigms, such keeping short the intervals between mammograms, using other modalities such as magnetic resonance imaging (MRI), or to signal the need for more careful interpretation of the mammogram, as double-reading. However, all these methods based on the radiologists' assessment present a major drawback: the subjectiveness in the categorization.

Computer-assisted measurement of breast density has been studied in the last few years in an attempt to obtain more objective risk assessments. Boyd et al. [8] proposed a semiautomatic method based on interactive thresholding which computes the percentage of the segmented dense tissue over the segmented breast area. Jamal et al. [13] described a similar technique and compared the semi-automatic assessment of breast density with Tabar patterns. Karssemeijer [14] developed an automated method where features are calculated from gray level histograms computed in different regions in which distance to the skin line is approximately equal, and then classified using the k -nearest neighbor (k -NN) rule. Saha et al. [15] described a method using a scale-based fuzzy connectivity approach. Klifa [16] et al. developed a segmentation technique based in fuzzy clustering to quantify breast density from MRI data. Oliver et al. [17] suggested an approach based on gross segmentation and the extraction of texture features of pixels with similar tissue appearance. This work was extended in [18] where a Fuzzy C-Means clustering approach was used for gross segmentation. Muhimmah et al. [19] used a feature extraction scheme based on a multiresolution histogram.

Segmentation of non-fatty tissue in mammograms appears to be more difficult than one might think, due to large differences in appearance between different parenchymal types [14]. In this sense, global thresholding techniques give limited results as mammograms differing in their density can present similar global histograms and vice versa.

Our approach is based on local gray-level histograms and on a two-stage classification scheme.

2 Dataset

In this work, the Mammographic Image Analysis Society (MIAS) Database [20] has been used both to train and to evaluate the proposed method according to a leave-one-out scheme.

The MIAS database contains 322 mammograms corresponding to the left and right breasts of 161 patients. Each image has a resolution of $200\mu m$ per pixel and a size of 1024×1024 pixels. Mammograms have been subjectively classified by a radiologist as *fatty* (F), *glandular* (G) and *dense* (D), according to its parenchymal tissue. This classification is what we consider the ground-truth. From the 322 mammograms that contains the dataset, 106 correspond to class F , 104 to G and 112 to D . Figure 1 shows a mammogram of each class.

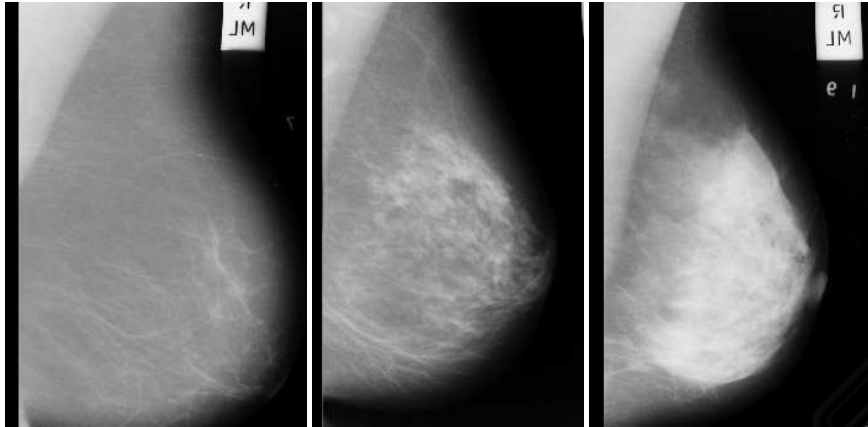


Fig. 1. Three mammograms of different types in the MIAS dataset. (a) Fatty, (b) Glandular, (c) Dense. The images have been cropped to show the region of interest.

It must be mentioned that this classification approach differs from that of Wolfe [6], Tabar [11], Boyd [8] and BI-RADS [12] presented at section 1 which all used four or more classes.

Fatty and dense tissue areas have not been segmented in each mammogram during the labeling process. Instead, a single global label is assigned to the whole mammogram.

3 Methodology

As mentioned before, only a single class label (F, G or D) is specified for each mammogram. This means that ground-truth at pixel level (or local level) is not available and therefore it is not possible to use a supervised method based on local features to train the classifier. On the other hand, methods based only on global features tend to fail due to high intraclass variability. In our approach, an unsupervised method for training with local features, which assigns local labels to each region of the mammogram is used. Then a supervised method where each mammogram is globally represented by a histogram of local labels is applied. This process is shown in Figure 2.

In a first process, the breast is manually segmented from the background of the mammogram. In this process, the breast is separated from other objects present in the mammography: black background, labels and the pectoral muscle. Although this can be automatically performed [14], in this work we have relied on a manual segmentation to avoid any contribution of segmentation errors to the results.

In the training phase, local features are first extracted from each image in the training set. For this purpose, a local window of 40×40 pixels is shifted along the breast region and the gray level histogram is computed at each position of the window, producing a *local feature vector* for each local window. To make these features invariant to acquisition parameters, breast thickness or other factors non-related with parenchymal type, histograms are stretched over the range $[0 - 31]$. With this operation we give

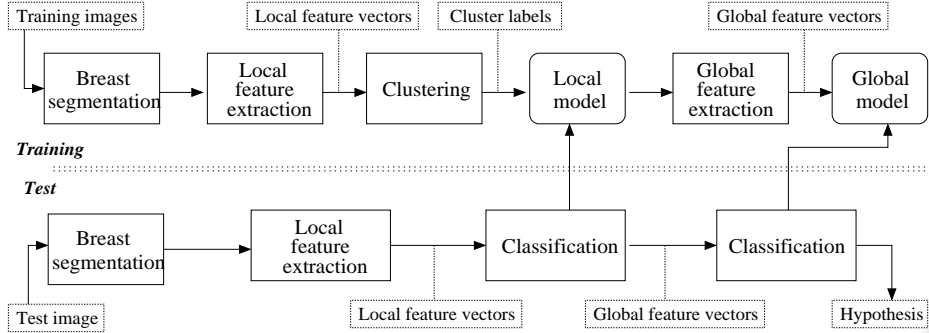


Fig. 2. Training and testing approaches proposed. In the first stage of training, local features are extracted, and an unsupervised approach is used, whereas in the second stage global features are extracted and a supervised method is applied. In the testing phase, a two-stage classification scheme is used, firstly, to switch from local to global features and then to obtain a hypothesis.

more relevance to the contrast between different textures in the local window, rather than the average gray level. In addition, histograms are conveniently reduced from 256 to 32 – *dimensional* feature vectors to limit the contribution of noise and the intraclass variance.

Then, the set of all local feature vectors is partitioned into n clusters using the k -means algorithm. This yields what we call the *local model*. Finally, the number of local feature vectors belonging to each cluster is computed for each mammogram. This yields an n -dimensional vector per mammogram, representing the normalized n -clusters histogram. This is what we call the *global features* vector of the mammogram and the set of all these vectors gives rise to the *global model*.

In the test phase, local feature vectors are computed in the same way as in the training phase. Then, local vectors are classified against the local model using the k -nearest neighbors (k -nn) rule, which assigns a cluster label to each vector. Next, cluster labels are counted to generate the normalized n -clusters histogram (global feature vector). Finally, this vector is classified against the global model using the k -nn rule again, which gives an F-G-D hypothesis.

4 Experiments and Results

For the evaluation of the performance of our approach, the whole set of 322 mammograms in the MIAS database was used. A leaving-one-patient-out technique has been employed, guaranteeing that when a mammogram is being classified, all the prototypes belonging to the same patient are left out from the training set.

Experiments were carried out for different number of clusters. The best results were obtained with 6 clusters. According to the classification in one of the three aforementioned classes determined by a radiologist, a success rate of 77.96% was obtained. The “Major classification error rate” (confusion between classes F and D) was only 1.24%. Among *major errors*, 75% (3 out of 4) are due to misclassifying a dense mammogram in class F , while 25% (1 out of 4) are due to misclassifying a fatty mammogram in class

D. It must be said that, in a practical task consisting of detecting specifically the images of dense breasts, misclassifying a dense mammogram in class F would be more serious than misclassifying a fatty mammogram in class D.

Table 1 shows the confusion matrix obtained. Rows represent the hypothesis and columns the ground truth.

Table 1. Confusion matrix for automatic classification and MIAS groundtruth.

	Fatty	Glandular	Dense
Fatty	94	8	3
Glandular	11	67	19
Dense	1	29	90

Our approach has been compared with other published results using the MIAS database. Table 2 summarizes these results. Muhimmah et al. [19] used a multiresolution histogram technique and a Directed Acyclic Graph - Support Vector Machine (DAG-SVM) classifier. Oliver et al. [17] used a method based on gross segmentation and the extraction of texture features of pixels with similar tissue appearance. A Decision Tree was employed for classification. Masek et al. [21] used average histograms of each density class as features and a Euclidean distance measure.

Table 2. Comparison with published results using the MIAS database.

Author	Agreement (%)	Major errors (%)
Our approach	77.96	1.24
Muhimmah et al.	77.57	3.43
Oliver et al.	70.0	4.44
Masek et al.	62.42	—

Our method outperforms the existing techniques tested with the MIAS database, and more importantly, major errors have been drastically reduced, which suggests that most of the minor errors could be attributed to mammograms whose density are actually in the frontier between two classes.

Also radiologists are reported to disagree on classifications. Some studies have found an inter-observer agreement of 66 to 80% [14, 18] in a 4-class test. Therefore, a significantly higher agreement using automatic classification is probably not to be expected.

5 Conclusions

Experiments of classification of mammographic density using local gray-level histograms and a two-stage classification scheme are presented. Using 322 images from the Mammographic Image Analysis Society (MIAS) Database in a 3-class leaving-one-out test, the results of 77.96% of agreement and 1.24% of major errors show an improvement

over other existing techniques. These results are probably at the same level that could be expected for expert manual classification.

References

1. E.J. Feuer, L.M. Wun: DEVCAN: Probability of Developing or Dying of Cancer. Version 4.0. Bethesda MD: National Cancer Institute. (1999)
2. A.M. Knutzen, J.J. Gisvold: Likelihood of malignant disease for various categories of mammographically detected, nonpalpable breast lesion. *Mayo Clin Proc*, Vol. 68 (1993) 454–460
3. D.B. Kopans: The positive predictive value of mammography. *AJR*, Vol. 158 (1992) 521–526
4. G.M. te Brake, N. Karssemeijer: Automated detection of breast carcinomas that were not detected in a screening program. *Radiology*, Vol. 207 (1998) 465–471
5. M. Wallis, M. Walsh et al.: A review of false negative mammography in a symptomatic population. *Clin Radiol* Vol. 44 (1991) 13–15
6. J.N. Wolfe: Breast pattern as an index of risk for developing breast cancer. *AJR*, Vol. 126 (1976) 1130–1139
7. J.N. Wolfe: Risk for breast cancer development determined by mammographic parenchymal pattern. *Cancer*, Vol. 37 (1976) 2486–2492
8. N.F. Boyd, J.W. Byng, R.A. Jong, et al.: Quantitative classification of mammographic densities and breast cancer risk: Results from the Canadian national breast screening study. *J. Nat. Cancer Inst.*, Vol. 87 (1995) 670–675
9. A.F. Saftlas, R.N. Hoover, L.A. Brinton, et al.: Mammographic densities and risk of breast cancer. *Cancer*, Vol. 67 (1991) 2833–2838
10. C. Byrne, C. Schairer, J.N. Wolfe, et al.: Mammographic features and breast cancer risk: Effects with time, age and menopause status. *J. Nat. Cancer Inst.*, Vol. 87 (1995) 1622–1629
11. I.T. Gram, E. Funkhouser, L. Tabar: The Tabar classification of mammographic parenchymal patterns. *Eur. J. Radiol.*, Vol. 124, (1997) 131–136
12. American College of Radiology (ACR): Illustrated Breast Imaging Reporting and Data System (BI-RADS). 3rd edn. Reston, VA: American College of Radiology, (1998) 167–181/
13. N. Jamal, K.H. Ng, L.M. Looi, et al.: Quantitative assessment of breast density from digitized mammograms into Tabar's patterns. *Phys. Med. Biol.*, Vol. 51 (2006) 5843–5857
14. N. Karssemeijer: Automated classification of parenchymal patterns in mammograms. *Physics in Medicine and Biology*, Vol. 43 (1998) 365–378
15. P.K. Saha, J.K. Udupa, E.F. Conant, D. Sullivan: Breast tissue density quantification via digitized mammograms. *IEEE Trans. on Medical Imaging*, (8) Vol. 20 (2001) 792–803
16. C. Klifa, J. Carballido-Gamio, L. Wilmes, et al.: Quantification of breast tissue index from MR data using fuzzy clustering. *Proceedings of the 26th Annual International Conference of the IEEE EMBS, San Francisco, CA, USA (2004) 1667–1670*
17. A. Oliver, J. Freixenet, A. Bosch, et al.: Automatic classification of breast tissue. *Lecture Notes in Computer Science*, Vol. 3523 (2005) 431–438
18. A. Oliver, J. Freixenet, R. Martí, et al.: A novel breast tissue density classification methodology. *IEEE Trans Inf Technol Biomed.*, Vol. 12 (2008) 55–65
19. I. Muhimmah, R. Zwigelaar: Mammographic density classification using multiresolution histogram information. *Proceedings of the International Special Topic Conference on Information Technology in Biomedicine*, (2006)
20. J. Suckling, J. Parker et al.: The mammographic images analysis society digital mammogram database. *Excerpta Medica. International Congress Series*, Vol. 1069 (1994) 375–378
21. M. Masek, S.M. Kwok, C.J.S. deSilva et al.: Classification of mammographic density using histogram distance measures. *Proceedings of the World Congress on Medical Physics and Biomedical Engineering*, (2003)